Soft X-ray Induced Decomposition of Phenylalanine and Tyrosine: A Comparative Study

Yan Zubavichus,*,†,‡ Michael Zharnikov,† Andrey Shaporenko,† Oliver Fuchs,§ Lothar Weinhardt,§ Clemens Heske,§,⊥ Eberhard Umbach,§ Jonathan D. Denlinger,|| and Michael Grunze†

Angewandte Physikalische Chemie, University of Heidelberg, INF 253, 69120 Heidelberg, Germany, Institute of Organoelement Compounds, Russian Academy of Sciences, 28 Vavilova Street, 119991 Moscow, Russia, Experimentelle Physik II, University of Würzburg, Am Hubland, 97074 Würzburg, Germany, Department of Chemistry, University of Nevada, 4504 Maryland Parkway, Las Vegas, Nevada 89154, and Advanced Light Source, 1 Cyclotron Road, Berkeley, California 94720

Received: February 11, 2004; In Final Form: March 25, 2004

The pristine state and soft X-ray induced decomposition of two aromatic amino acids, viz. phenylalanine and tyrosine, have been studied by means of XPS and NEXAFS. The spectroscopic data on radiation induced decomposition have been supplemented by a mass spectral analysis of the desorbed species. Despite very similar chemical structures, the two amino acids show a dramatically different behavior toward ionizing radiation: phenylalanine degrades very quickly whereas tyrosine shows a prominent stability against radiation damage. Reasons for this difference are discussed in relation to radical-mediated reactions responsible for the decomposition.

1. Introduction

The decomposition of organic molecules under the impact of electrons or photons (in a wide spectral range from the UV to γ-radiation) and the desorption of their fragments has attracted a lot of attention in recent years, emerging into a field often referred to as DIET (desorption induced by electronic transitions).[1−5] Problems of radiation sensitivity are especially severe for samples of biological origin.[6] The molecular mechanisms of irradiation-induced degradation of biological macromolecules have been considered in numerous studies applying different analytical techniques, including electron paramagnetic resonance (EPR) spectroscopy and its modifications (e.g., electron nuclear double resonance, or ENDOR),[7−16] mass spectrometry,[17−22] X-ray photoelectron spectroscopy (XPS),[23] electron energy loss spectroscopy (EELS),[24,25] electron and X-ray diffraction,[26−28] and many others. Nevertheless, many fundamental aspects of the decomposition reactions remain largely unexplored.

In an earlier paper,[29] the decomposition of five aliphatic amino acids in the solid state (viz. alanine, serine, cysteine, aspartic acid, and asparagine), induced by irradiation with soft X-rays, was studied under ultrahigh vacuum (UHV) conditions by means of XPS, near-edge X-ray absorption fine structure (NEXAFS) spectroscopy, and mass spectrometry. In particular, it was found that these substances decompose under irradiation via several competing pathways, including dehydrogenation, decarboxylation, deamination, and dehydration. Qualitatively, the above five amino acids were arranged in the following series of increasing radiation stability: serine < alanine < aspartic acid < cysteine < asparagine. In the current paper, we extend that study to two aromatic amino acids, L-phenylalanine (Phe) and L-tyrosine (Tyr), which are described by very similar molecular formulas as shown in Figure 1. L-Tyrosine merely differs from L-phenylalanine by an OH substituent in the para position of the phenyl ring. In addition to the study of the different radiation-induced decomposition paths of the two amino acids, their pristine states are carefully characterized with XPS and NEXAFS spectroscopies.

Phenylalanine (Phe) Tyrosine (Tyr)

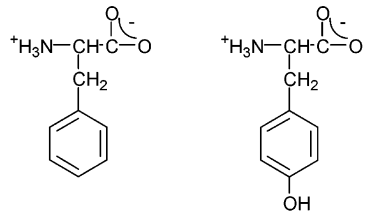

Figure 1. Molecular formulas of phenylalanine and tyrosine in the zwitterionic state.

2. Experimental Section

The experimental approach used to study the decomposition of amino acids under soft X-ray irradiation has been comprehensively described in our earlier paper.[29] Thus, only essential details will be outlined here.

Commercially available polycrystalline powders of phenylalanine and tyrosine (Sigma-Aldrich or Alfa Aesar, purity > 98%) were finely ground (down to the grain size of a few micrometers) and pressed into Ar^+-sputter-cleaned indium foil. The samples were loaded into a UHV chamber, pumped down to the pressure of ca. 5×10^{-10} mbar, and then exposed to soft X-rays. All spectra were taken at room temperature.

For XPS and mass spectral data collection, the radiation was produced by a Mg Kα X-ray source, operated at 300 W (15 kV $\times$ 20 mA) and positioned about 20 mm in front of the sample

* To whom correspondence should be addressed. E-mail: yan.zubavichus@urz.uni-heidelberg.de.
† University of Heidelberg.
‡ Institute of Organoelement Compounds.
§ University of Würzburg.
⊥ Department of Chemistry, University of Nevada.
|| Advanced Light Source.

10.1021/jp049376f CCC: $27.50
Published on Web 04/27/2004

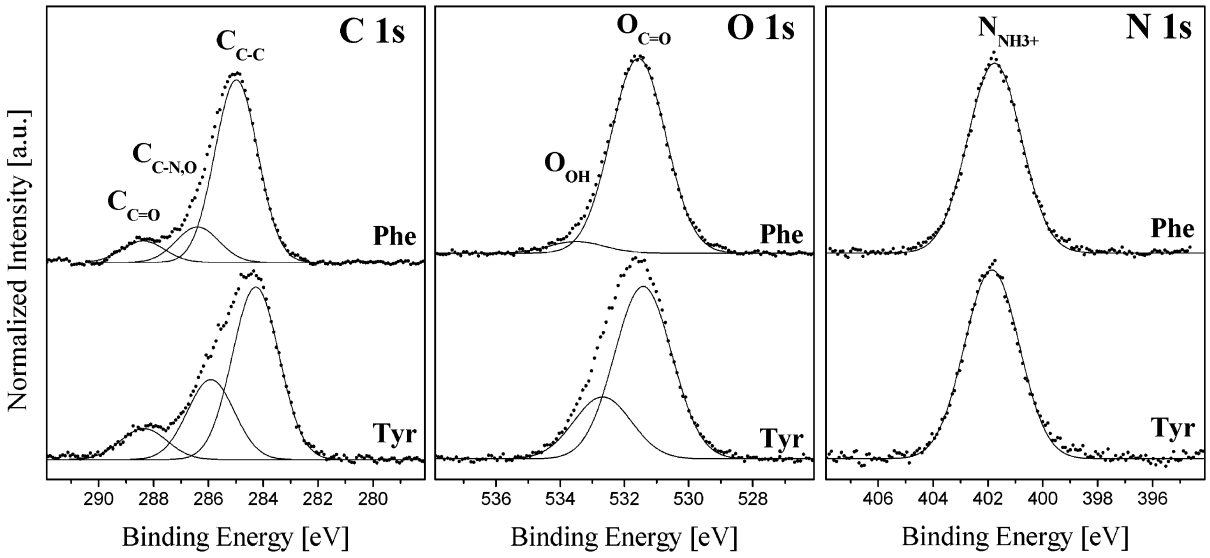

Figure 2. C 1s, O 1s, and N 1s XPS spectra of phenylalanine (Phe) and tyrosine (Tyr): experimental data (dots) and peak fit results (solid lines).

surface. Owing to the constant geometry and operation parameters of the X-ray source, the radiation dose absorbed by the samples is proportional to the exposure time. The maximum exposure time was 5−6 h. X-ray photoelectron spectra in the regions of the C 1s, N 1s, and O 1s core levels were measured using a VG ESCAscope spectrometer[30] in the fixed analyzer transmission (FAT) mode with a pass energy of 40 eV. For a quantitative analysis, XPS spectra were background-subtracted using polynomial functions, fitted using symmetrical Gaussian functions, and integrated. Standard atomic sensitivity factors[31] empirically corrected for the analyzer transmission were used. The overall accuracy of the quantitative analysis is estimated to 10−15%. At the same time, the quantification of irradiation-induced relative changes in the XPS spectra is precise within 1−2% since it is defined by the experimental signal-to-noise ratio. To compensate for charging effects, the binding energy (BE) scale was adjusted to provide a BE of 288.4 eV for the C 1s feature corresponding to carbon atoms of the carboxyl groups.[29,32] Mass spectra were recorded simultaneously with the XPS spectra every 10−15 min using a Transpector residual gas analyzer (electron impact ionization at 102 eV, analysis of positive ions from 0 to 200 amu). The detection limit of the electron multiplier detector of the gas analyzer is around 10^{-13} A.

C, N, and O K-edge NEXAFS spectra for pristine amino acids were taken at the bending magnet HE-SGM beamline of the synchrotron radiation facility BESSY II (Berlin, Germany). The spectra were acquired in the partial electron yield (PEY) mode using a channelplate detector with a threshold voltage of 150 V (C K-edge), 300 V (N K-edge), or 350 V (O K-edge) and normalized to a reference spectrum of clean gold measured in an independent run. The scanning step was varied from 0.1 eV in the region of narrow spectral features to 0.2−0.5 eV in the preedge and postedge regions. The acquisition time was 3−4 min per spectrum. No spectral changes were observed in the series of several consecutive scans, indicating that these spectra are characteristic of the pristine amino acids. Other parameters of the measurements may be found elsewhere.[33]

Along with the PEY spectra, NEXAFS spectra in the total fluorescence yield (TFY) mode were also acquired. The measurements were performed at the undulator beamline 8.0 of the Advanced Light Source (Lawrence Berkeley National Laboratory, Berkeley, CA). The fluorescence intensity was measured with a negatively biased (ca. 1 kV) channeltron detector and then normalized to the simultaneously measured reference current from a grid of freshly evaporated gold placed in the primary X-ray beam before the sample. In addition, taking advantage of the high photon flux at this beamline, time-resolved series of NEXAFS spectra were taken in order to monitor radiation-induced changes. At each edge, 10−15 consecutive scans were recorded with an energy step of 0.05 eV (region of π^*-resonances in C K-edge spectra) or 0.2 eV (N and O K-edges) and a dwell time of 0.5−2 s per point, resulting in an overall acquisition time of 1−2 min for each spectrum. The first spectra of each series were taken on previously unexposed spots of the sample. For the two amino acids, the photon fluxes are estimated to be equal within 15−20%.

3. Results

3.1. NEXAFS and XPS Characterization of Pristine Phenylalanine and Tyrosine. *3.1.1. XPS Results.* Initial XPS spectra of the two amino acids in the C 1s, N 1s, and O 1s regions are depicted in Figure 2. The peak fit for the C 1s spectra gives three major components, in agreement with the molecular formulas of phenylalanine and tyrosine (see Figure 1) and results of earlier XPS studies on amino acids.[29,32] The three components correspond to carbon atoms of the carboxyl groups at 288.4 eV (denoted as $C_{C=O}$ in left panel in Figure 2), carbon atoms functionalized with hydroxy or amino groups centered at ca. 287 eV (denoted as $C_{C-N,O}$), and other carbon atoms without strong electronegative substituents (denoted as C_{C-C}) around 285 eV. Similarly, O 1s core-level spectra (central panel of Figure 2) were fitted using two components, corresponding to keto oxygen ($O_{C=O}$) of the carboxyl group at ca. 531.4 eV (for the zwitterionic form of amino acids, both oxygen atoms of a deprotonated carboxyl group are chemically identical and contribute to the signal at this binding energy) and to the hydroxyl oxygen (O_{OH}) at ca. 532.7 eV. Only one component at ca. 401.7 eV is sufficient to describe the N 1s spectra (right panel of Figure 2) of pristine phenylalanine and tyrosine, which is assigned to protonated amino groups ($N_{NH_3^+}$).

The results of a quantitative analysis of the XPS spectra for the pristine amino acids are shown in Table 1, in comparison with the nominal stoichiometry and stoichiometries of the samples exposed to X-rays for different durations (to be discussed below). The intensity ratios between the individual

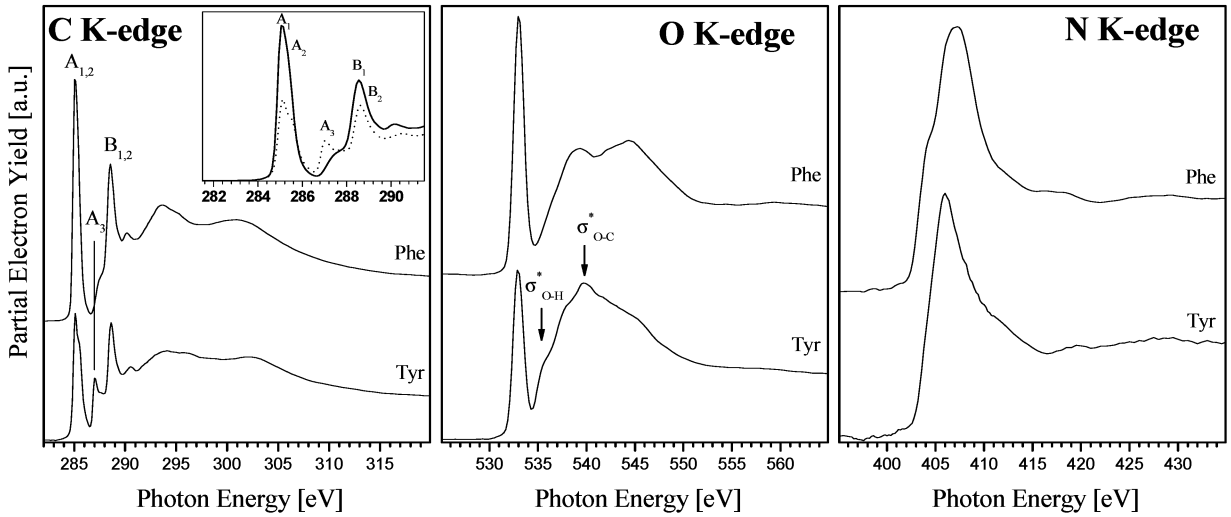

Figure 3. Partial electron yield NEXAFS spectra of pristine phenylalanine (Phe) and tyrosine (Tyr) at the C (left panel), O (central panel), and N K-edge (right panel). The inset to the C K-edge spectrum shows the zoomed region of the π^*-resonances: phenylalanine (solid line) and tyrosine (dots).

TABLE 1: Results of a Quantitative XPS Analysis (at. %) for Phenylalanine (Phe) and Tyrosine (Tyr): Nominal Stoichiometry, Pristine State, and After Specified Durations (in min) of Exposure to Soft X-rays[a]

		C_{C-C}	$C_{C-N,O}$	$C_{C=O}$	C	$O_{C=O}$	O_{OH}	O	$N_{NH_3^+}$ [b]	N_{NH_2}	N
Phe	stoichiometry	58.3	8.3	8.3	75.0	16.7	0	16.7	8.3	0	8.3
	pristine	64.5	6.8	6.5	77.8	12.2	0.7	12.9	9.0	0.4	9.4
	50 min	66.8	10.0	4.8	81.3	10.1	0.7	10.8	6.7	1.1	7.8
	120 min	76.4	8.7	2.1	87.2	6.0	0.8	6.8	2.9	3.1	6.0
	240 min	88.7	3.8	0	92.5	2.1	0.7	2.8	1.0	3.6	4.6
Tyr	stoichiometry	46.2	15.4	7.7	69.2	15.4	7.7	23.1	7.7	0	7.7
	pristine	42.5	19.6	7.9	70.0	14.9	5.1	20.0	10.0	0.0	10.0
	70 min	45.9	20.7	6.3	72.9	13.4	5.1	18.5	7.8	0.8	8.6
	150 min	45.2	21.8	5.9	72.9	13.5	5.3	18.8	7.2	1.1	8.3
	290 min	49.4	20.5	4.8	74.6	11.7	6.2	17.9	6.0	1.5	7.5

[a] Notations of components used in the fitting are explained in the text and shown for the pristine amino acids in Figure 2. [b] For the calculations of the stoichiometric $N_{NH_3^+}$ fractions, phenylalanine and tyrosine are assumed to be 100% zwitterionic.

components in the O 1s and N 1s spectra confirm that the zwitterionic state dominates at the surface of the pristine amino acid crystallites. The slight differences between the actual peak intensities and the stoichiometric ratios are within normal error bars; they are mainly due to inaccuracies of the fit procedure and of the sensitivity factors and transmission corrections.

3.1.2. NEXAFS Results. C, N, and O K-edge NEXAFS spectra of pristine phenylalanine and tyrosine, measured using the PEY acquisition mode, are shown in Figure 3. C K-edge spectra of both amino acids (left panel of Figure 3) exhibit similar well-developed fine structures with many sharp spectral features. Both the energy positions of these features and general spectral shapes are similar to the transmission NEXAFS spectra of phenylalanine and tyrosine reported earlier by other authors.[34,35] The group of peaks labeled "A" originates from transitions of the C 1s electrons to antibonding π^*-orbitals associated with the substituted benzene rings of phenylalanine and tyrosine.[35,36] The component A_3, which is present only in the spectrum of tyrosine, is shifted from the main peak by ca. 2 eV due to the electronegative OH substituent. For instance, in the C K-edge ISEELS spectrum of gaseous phenol,[37] the analogous feature was found at 287.1 eV, which is 1.9 eV above the major π^*-transition. In the spectrum of phenylalanine, a shoulder is observed at slightly higher excitation energies, which corresponds to the position of the absorption edge (it is simulated well with an arctangent step function). The peak B corresponds to π^*-resonances of the carboxyl group.[35,36,38] For both amino acids, it has an asymmetric shape and can be fitted with two components (B_1 and B_2 in Figure 3). Broader features in the range of 290−310 eV are due to transitions of C 1s electrons to different antibonding σ^*-orbitals.

O K-edge NEXAFS spectra of phenylalanine and tyrosine (central panel of Figure 3) are dominated by a π^*-resonance of the carboxyl group at ca. 533 eV,[38,39] followed by a broad peak composed of several overlapping σ^*-contributions at 535−550 eV. Since the additional oxygen atom in the tyrosine molecule forms only σ-bonds, it contributes solely to the σ^*-region of the NEXAFS spectrum. As a result, the relative intensity of the σ^*-features is noticeably higher for tyrosine than for phenylalanine. Differences in the spectral shapes of the σ^*-regions between tyrosine and phenylalanine may be also attributed to the additional OH group. In particular, a shoulder at ca. 535 eV and a component at ca. 540 eV (marked with arrows in the central panel of Figure 3) are assigned to transitions of O 1s electrons to antibonding σ^*-orbitals with a dominant O−H and O−C character within the H−O−Ph moiety, respectively. For instance, in the O K-edge ISEELS spectrum of gaseous phenol, the respective features were found at 534.9 and 539.4 eV, respectively.[37]

N K-edge NEXAFS spectra of phenylalanine and tyrosine (right panel of Figure 3) show only broad σ^*-components. Surprisingly, the two spectra are noticeably different. In particular, the main component in the spectrum of phenylalanine has a broader and more asymmetric shape (with a shoulder at ca. 404.5 eV) as compared to that of tyrosine. Note that a sensitivity of N K-edge ISEELS spectra of substituted aniline

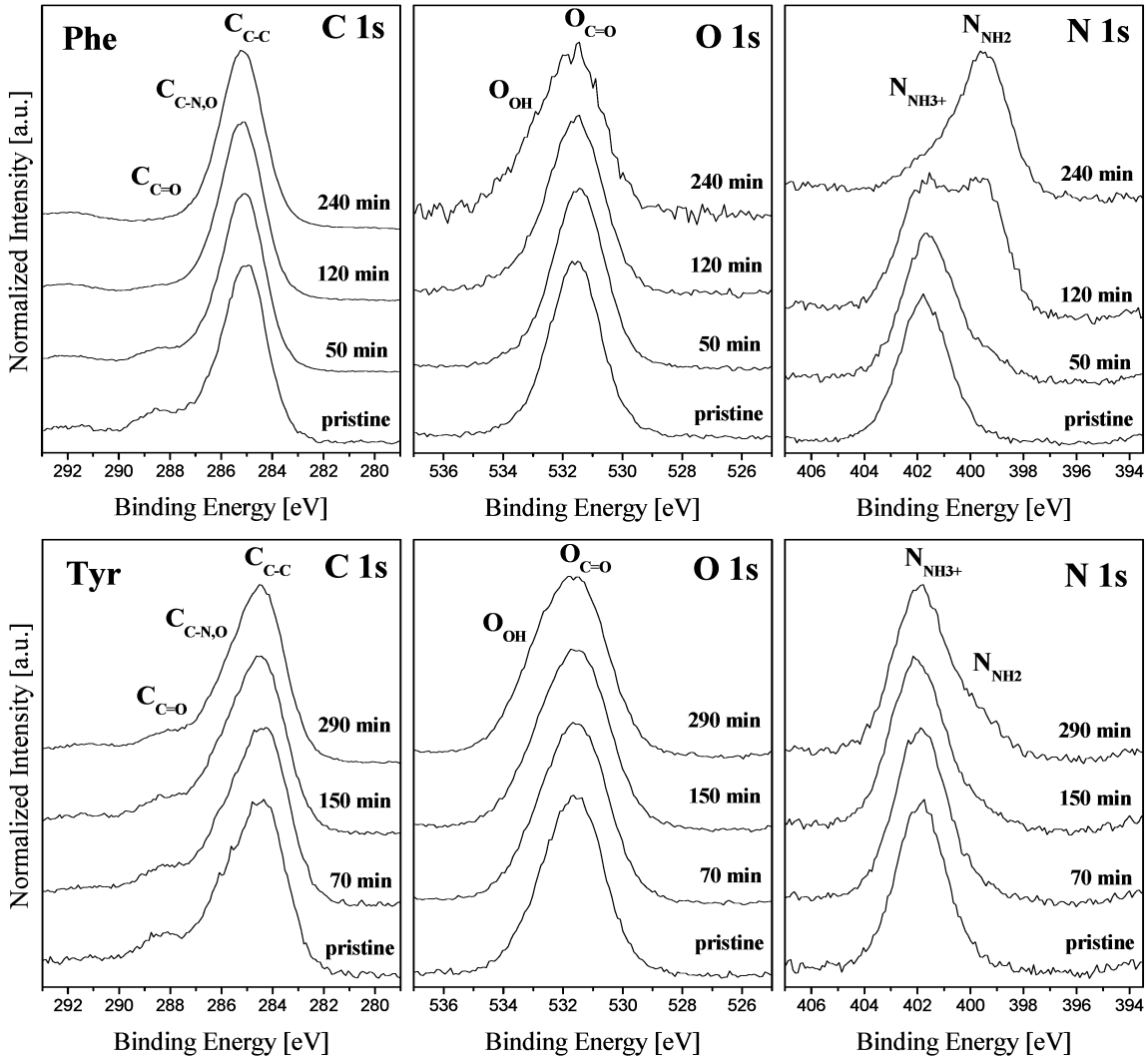

Figure 4. Time evolution of C 1s, O 1s, and N 1s XPS spectra of phenylalanine (Phe) and tyrosine (Tyr) during continuous exposure to soft X-rays.

to the charge transfer induced by a substitution within the benzene ring has been proven both experimentally and theoretically.[41] However, in our case it is hardly possible that a hydroxy group in the benzene ring of tyrosine may influence the chemical state of the N atom in the distant amino group this strongly. Though reasons for the difference are not fully understood presently, we suggest it may reflect different patterns of intermolecular contacts in crystalline structures of the two amino acids, which both form very strong H bonds.[42,43] A strong dependence of O K-edge NEXAFS spectra of ice and liquid water on the exact geometry of the H bonds has been recently demonstrated.[44] Another potentially important factor for the two amino acids is the balance between zwitterions and neutral molecules. Though XPS data for the pristine amino acids support the predominance of the zwitterionic form, the time-resolved results discussed below assume that phenylalanine rapidly converts from the zwitterionic to the neutral state under irradiation, suggesting that a protonation of the amino group is less favorable as compared to tyrosine.

3.2. Irradiation-Induced Processes in Solid Phenylalanine and Tyrosine. *3.2.1. Qualitative and Quantitative Changes in XPS Spectra.* The evolution of the C 1s, O 1s, and N 1s XPS spectra with irradiation time for phenylalanine and tyrosine is shown in Figure 4 (all spectra are normalized to the maximum intensity). The results of a quantitative data analysis are summarized in Table 1. For phenylalanine (three upper panels of Figure 4), the irradiation-induced changes may be summarized as follows:

1. The relative amount of carbon (C) increases from 78% to 93% at the cost of oxygen (a decrease from 13% to 3%) and nitrogen (a decrease from 9% to 5%).

2. The fraction of carboxyl-type carbon ($C_{C=O}$) decreases gradually with irradiation time and drops below the detection limit of the experimental setup after ca. 2 h of irradiation.

3. The $O_{C=O}$ component at high BE decreases significantly with respect to the O_{OH} component.

4. A new N 1s component, assigned to unprotonated amino groups[29,32] at a BE of ca. 400.0 eV, evolves and becomes dominant after about 2 h of irradiation.

Therefore, several chemical processes are initiated in phenylalanine by irradiation, similar to aliphatic amino acids studied earlier.[29] In particular, decarboxylation and deamination of phenylalanine evidently take place, leading to a significant enrichment of the sample's surface with hydrocarbon-like species (C_{C-C} component). Additionally, a fast deprotonation of the amino group occurs.

The radiation-induced changes in the C 1s, O 1s, and N 1s core-level XPS spectra of tyrosine during irradiation are shown in the three lower panels of Figure 4. While the spectra show tendencies similar to those of the spectra of phenylalanine, all

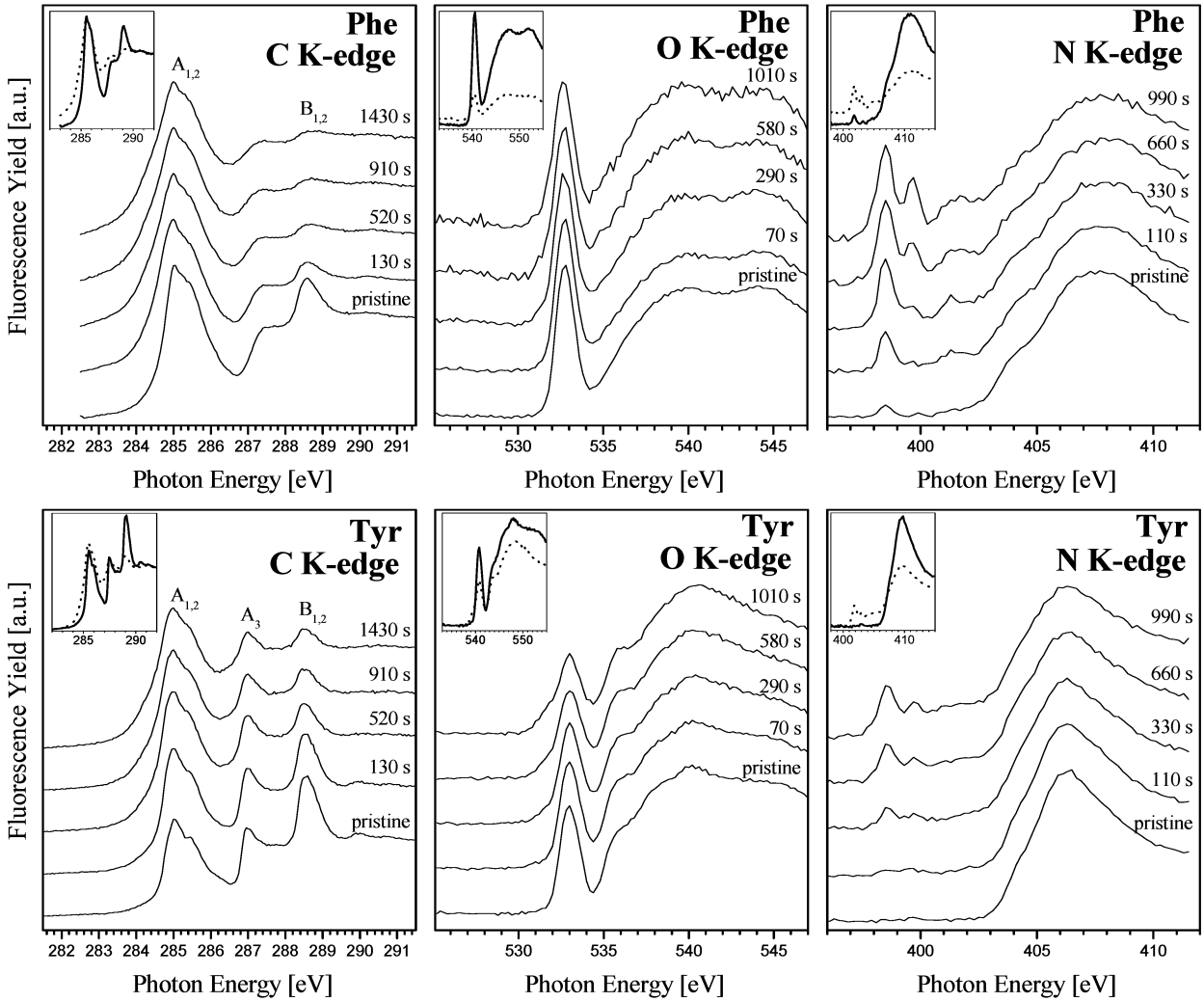

Figure 5. Time evolution of the total fluorescence yield NEXAFS spectra of phenylalanine (Phe) and tyrosine (Tyr) during continuous exposure to high-brilliance soft X-rays. Insets compare the first and last spectra of the series as measured without rescaling.

changes evolve much slower during irradiation (see also the quantitative analysis results in Table 1). In particular, the carboxyl component is still clearly distinguishable in the C 1s XPS spectrum of tyrosine after about 5 h of radiation exposure (its fraction decreases from ∼8% to ∼5%; see Table 1). Furthermore, the unprotonated amino group component (lower BE component at about 400.0 eV) in the N 1s spectrum is significantly less intense than the protonated amino group component, suggesting that the zwitterionic state of tyrosine is stable and remains dominant even after prolonged irradiation.

3.2.2. Evolution of NEXAFS Spectra. TFY NEXAFS spectra of phenylalanine and tyrosine at the C, N, and O K-edges measured using high-brightness undulator radiation are shown in Figure 5 as a function of irradiation time. The bottom spectra of each series corresponding to the least damaged samples (labeled "pristine") are very similar to the bending magnet PEY spectra of pristine amino acids discussed above and show the same characteristic spectral features of the two amino acids. Thus, the two acquisition modes with effective probing depths differing by more than 1 order of magnitude give fully consistent results.

Intense soft X-ray irradiation induces significant spectral changes for both amino acids on a time scale of several minutes. In the C K-edge spectra of irradiated samples, the spectral feature A becomes broader and asymmetric, which suggests an emergence of new spectral features in the energy range of 285−287 eV. Furthermore, the intensity of the feature B decreases prominently, which indicates a progressive decarboxylation in full agreement with the XPS results. In the case of phenylalanine, the carboxyl π^*-peak ($B_{1,2}$) at ca. 288.6 eV virtually disappears after irradiation of the sample for 15 min, while the analogous decrease for tyrosine is substantially smaller.

The shapes of the O K-edge NEXAFS spectra of phenylalanine and tyrosine (two central panels of Figure 5) do not change dramatically upon irradiation. The most prominent change is an overall decrease of intensity, which means that, upon irradiation, both samples lose oxygen (most probably through decarboxylation and dehydration). This process is much faster for phenylalanine—after ca. 17 min of irradiation, the oxygen-related signal diminishes by a factor of 2.5 to 3—whereas the respective decrease in the case of tyrosine is only 25−30%. Furthermore, a shoulder at 531−532 eV develops in both cases, which is especially prominent for tyrosine. We attribute this new feature to 1s→π^*(C═O) transitions associated with ketone- or aldehyde-like species (which are probably formed by dehydration of the carboxyl groups): these transitions are typically observed at energies 1−1.5 eV lower than corresponding carboxylic species.[38]

The most striking change in the nitrogen K-edge NEXAFS spectra (two right panels of Figure 5) is the development of new peaks, viz. two relatively narrow features at 398.5 and 399.7 eV, and a broader feature at ca. 401.5 eV. For phenylalanine,

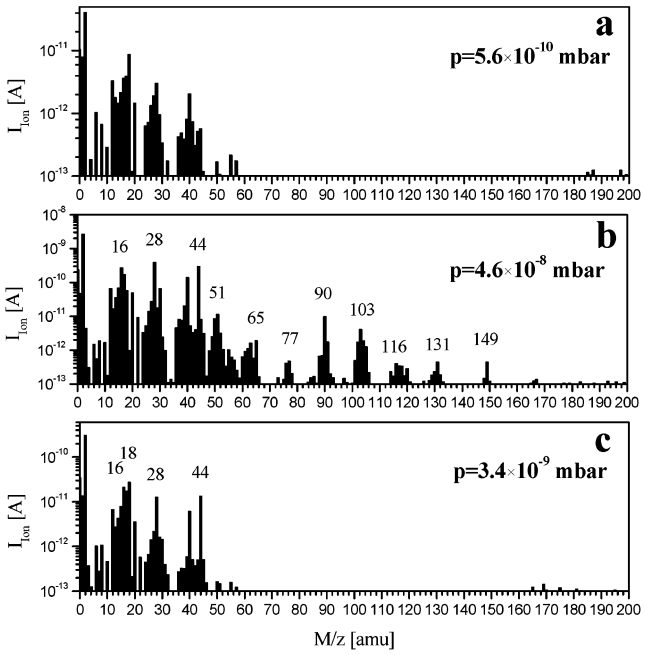

Figure 6. Mass spectral patterns of the UHV chamber: (a) typical residual gas pattern of the UHV chamber; (b) pattern after irradiation of phenylalanine for 270 min; (c) pattern after irradiation of tyrosine for 330 min.

these peaks, though very weak, are distinguishable already in the first scan of the series. These features evolve in the energy range typical of electronic transitions associated with unsaturated π-systems involving a nitrogen atom and are, therefore, indicative of a partial dehydrogenation of N-containing groups resulting in the formation of N═C and N≡C multiple bonds.[29] On the other hand, similar spectral features are often observed in ISEELS spectra of gaseous molecules containing NH_x groups ($x = 1-3$), such as ammonia, alkylamines, or glycine.[39,40] In those cases, the respective peaks are assigned to mixed Rydberg/σ^*_{N-H} transitions. In solid zwitterionic amino acids, such transitions are quenched (for instance, respective peaks disappear on going from gaseous to solid glycine[39]) due to the strong intermolecular bonds. Therefore, the emergence of new features in the energy range of 398−402 eV in N K-edge NEXAFS spectra of phenylalanine and tyrosine may be partly attributed to a disruption of extended three-dimensional networks of strongly interacting zwitterions with a formation of gaslike neutral molecules, which weakly interact with their neighbors. This interpretation is consistent with the changes observed in N 1s XPS spectra.

3.2.3. Compositional Changes of the Gas Phase as Monitored by Mass Spectrometry. A typical mass spectral pattern of the residual gas in the UHV chamber (a) is compared to the analogous MS spectra after prolonged exposures of phenylalanine (b) and tyrosine (c) to soft X-rays in Figure 6. In this figure, ion currents are plotted on a logarithmic scale to emphasize contributions of minor gaseous components. The dominant peaks in the mass spectral patterns correspond to the following masses: 2 (H_2), 16 (NH_2, O), 18 (H_2O), 28 (CO, H_2CN), and 44 (CO_2) amu. These peaks also show the most pronounced dynamics upon exposure, as shown in Figure 7. For phenylalanine (a), the NH_2 and CO_2 peaks show similarly fast increases in the initial stages of the irradiation while CO (or, partly, H_2CN) becomes the dominant species in the late stages. In the case of tyrosine (b), the changes in the ion currents are very weak. Apart from hydrogen, water shows the most prominent increase in the early stages and remains the dominant component, even though its signal starts to decrease after about 2 h of exposure.

An interesting pattern of higher mass ions ($m/z > 70$ amu) is observed in the case of phenylalanine (see central panel of Figure 6): it reveals a series of distinct and relatively intense peaks centered at (in descending order of their relative intensities) 90, 103, 77, 149, and 131 amu. A probable assignment of these peaks and their origins are discussed below. The peak corresponding to the molecular ion of phenylalanine ($M_w = 165$ amu) is also found, but its intensity is barely higher than the detection limit of the residual gas analyzer.

Our phenylalanine MS pattern is distinctly different from the one expected for gaseous phenylalanine under electron impact. The electron impact mass spectral pattern of the gaseous ethyl ester of phenylalanine (esters of amino acids have much higher volatility, so they are more easily studied with conventional mass spectrometry) is dominated by four peaks with the following masses: 120 (100), 102 (83), 74 (ca. 35), and 91 (23) (numbers

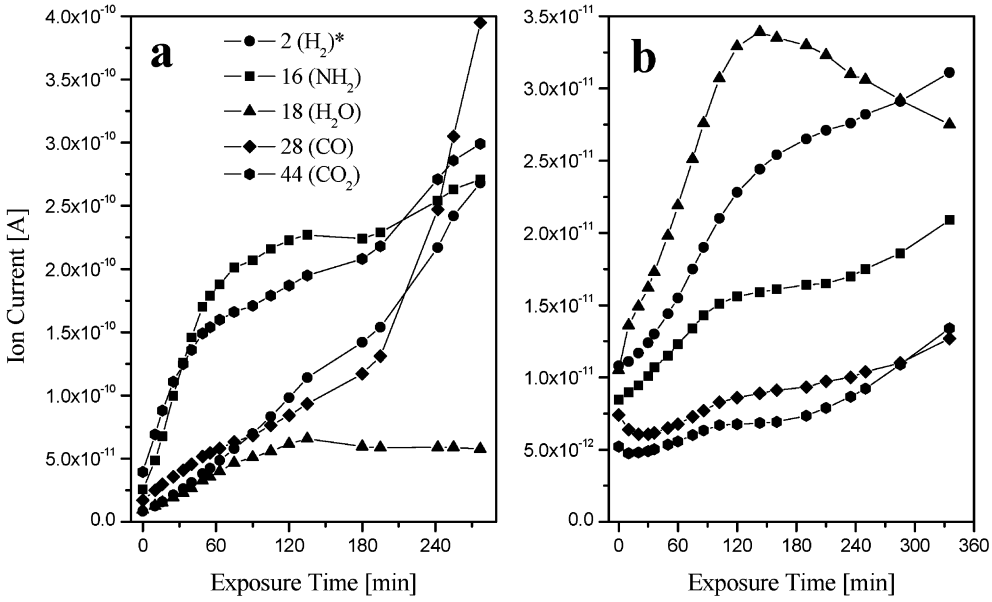

Figure 7. Concentration changes of principal residual gas components during X-ray exposure: (a) phenylalanine; (b) tyrosine. *Ion currents of H_2^+ ($m/z = 2$) are divided by 10.

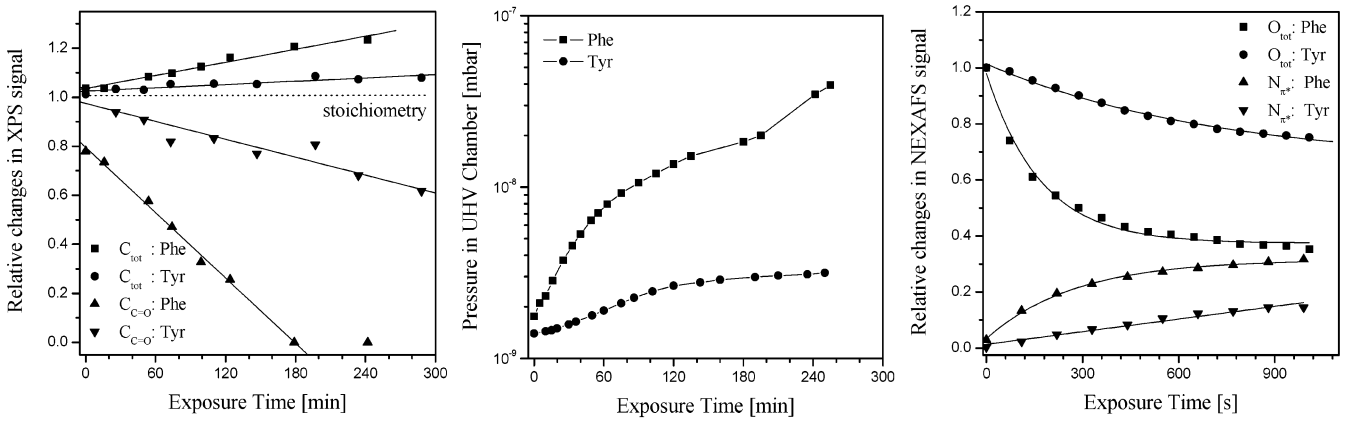

Figure 8. Semiquantitative characteristics of decomposition rates for phenylalanine and tyrosine. Left panel: changes in the molar fractions of the components C_{tot} and $C_{C=O}$ relative to the stoichiometry with exposure time according to the quantitative analysis of the XPS data. Central panel: total pressure increase in the main UHV chamber during exposure of phenylalanine and tyrosine to soft X-rays (1253.6 eV, 15 kV, 20 mA). Right panel: decrease of the integral intensity of the O K-edge NEXAFS signal (O_{tot}) and increase of the integral intensity of the π^*-resonances (396−403 eV) relative to the total integral intensity of the N K-edge NEXAFS signal (N_{π^*}).

in parentheses denote the relative intensities of the respective peaks).[45] These peaks are assigned to $[PhCH_2CHNH_2]^+$, $[NH_2CHCOOEt]^+$, $[COOEt]^+$, and $[PhCH_2]^+$ ions.[45] This assignment indicates that, under electron impact in the ionizer of the mass spectrometer, the phenylalanine derivative undergoes a fragmentation via two major pathways: decarboxylation and a scission of the $C_\alpha-C_\beta$ bond resulting in a detachment of the glycine-like fragment and a formation of the benzyl cation. As a result, the molecular ion peak has an intensity of only 1 (i.e., 1% of the dominant peak at 120 amu).

In the pattern shown in Figure 6, the peak at 120 amu is very weak (only ∼3% of the strongest peak at 90 amu). Therefore, the effects of X-ray irradiation on polycrystalline powder of phenylalanine cannot be reduced to a simple thermally or radiation stimulated desorption of intact molecules (taking into account the low relative intensity of the respective molecular ion peak, this suggestion cannot be ruled out a priori). Thus, the aforementioned higher mass ions appear in the MS pattern as a result of X-ray induced decomposition and desorption of fragments smaller than the intact phenylalanine molecule (see discussion below).

4. Discussion

XPS, NEXAFS, and mass spectrometry provide complementary insights into radiation-induced processes in the two amino acids. Some quantitative characteristics of the decomposition rates as monitored by the three experimental techniques are shown in Figure 8. Notably, all three methods consistently indicate that tyrosine is substantially more stable than phenylalanine, i.e., that the substitution of an H atom by an OH group in the benzene ring of phenylalanine leads to a pronounced stabilization of the whole amino acid molecule. In contrast, in our previous study,[29] we found that serine (OH-substituted alanine) was less stable than alanine. Moreover, the OH group was shown to be the "weakest point" of serine, since the dominant decomposition pathway was a dehydration through scission of the C−OH bond.

Therefore, the effect of specific functional groups (in this case, introduction of an OH group) on the radiation stability of the target molecule may be quite different depending on the position of the functionalization (aliphatic chain or aromatic ring). Thus, the simple "building block" principle, which considers a molecule as a linear superposition of its constituents, requires great care if applied for an evaluation of the radiation stability of amino acids.

The pronounced stability of tyrosine with respect to phenylalanine should be closely related to the OH substitution. Indeed, it is known that a dehydrogenation of the OH group in tyrosine leads to the formation of a very stable radical with an unpaired electron delocalized over the oxygen atom and the six carbon atoms of the benzene ring.[46] Such long-lived tyrosyl radicals play a crucial role in many biochemical reactions with a participation of proteins and, primarily, in photosynthesis.[47,48] Tyrosyl radicals can be generated by radiolysis (with UV or γ-radiation) or a mild chemical oxidation of tyrosine.[49] In particular, tyrosyl radicals are generated as the major paramagnetic product by irradiating tyrosine single crystals with γ-rays at low temperatures, as evidenced by electron paramagnetic resonance (EPR) spectroscopy.[8,9,13] Furthermore, it was suggested that the tyrosine residue can serve as a radical sink in larger protein molecules; i.e., electron deficiencies are transferred from primary excitation centers to tyrosine along the peptide chain.[50] Since formation of the tyrosyl radical does not result in an immediate fragmentation of the whole molecule (parent tyrosine can be easily restored by the attachment of an H atom), the presence of a tyrosine residue has a stabilizing effect to other parts of the protein.[10]

Notably, γ-irradiation of phenylalanine single crystals under similar conditions leads to the formation of benzyl radicals,[8,11] i.e., a defragmentation of the parent molecule. Formation of benzyl radicals under irradiation of phenylalanine with electrons was also suggested on the basis of EELS data.[24] As has been already noted above, benzyl cations are formed upon electron impact ionization of phenylalanine, as detected by mass spectrometry.[44]

Taking into account all the experimental evidence considered above, we suggest the following qualitative scheme of processes initiated in the two aromatic amino acids by soft X-ray irradiation (Figure 9). The first step is induced by the primary excitation. The major channel of the primary excitation is the photoionization due to the absorption of a soft X-ray photon leading to the creation of a core hole. Due to the local nature of the core excitation, each atom of the organic molecule can be ionized with a probability proportional to the photoionization cross section of the respective element. Other minor excitation channels include shake-up and shake-off processes and, probably, interaction of the molecules with secondary electrons, i.e., inelastic scattering and attachment of electrons.

The excitation into antibonding or nonbonding orbitals as well as the relaxation of the excited state (for instance, through an

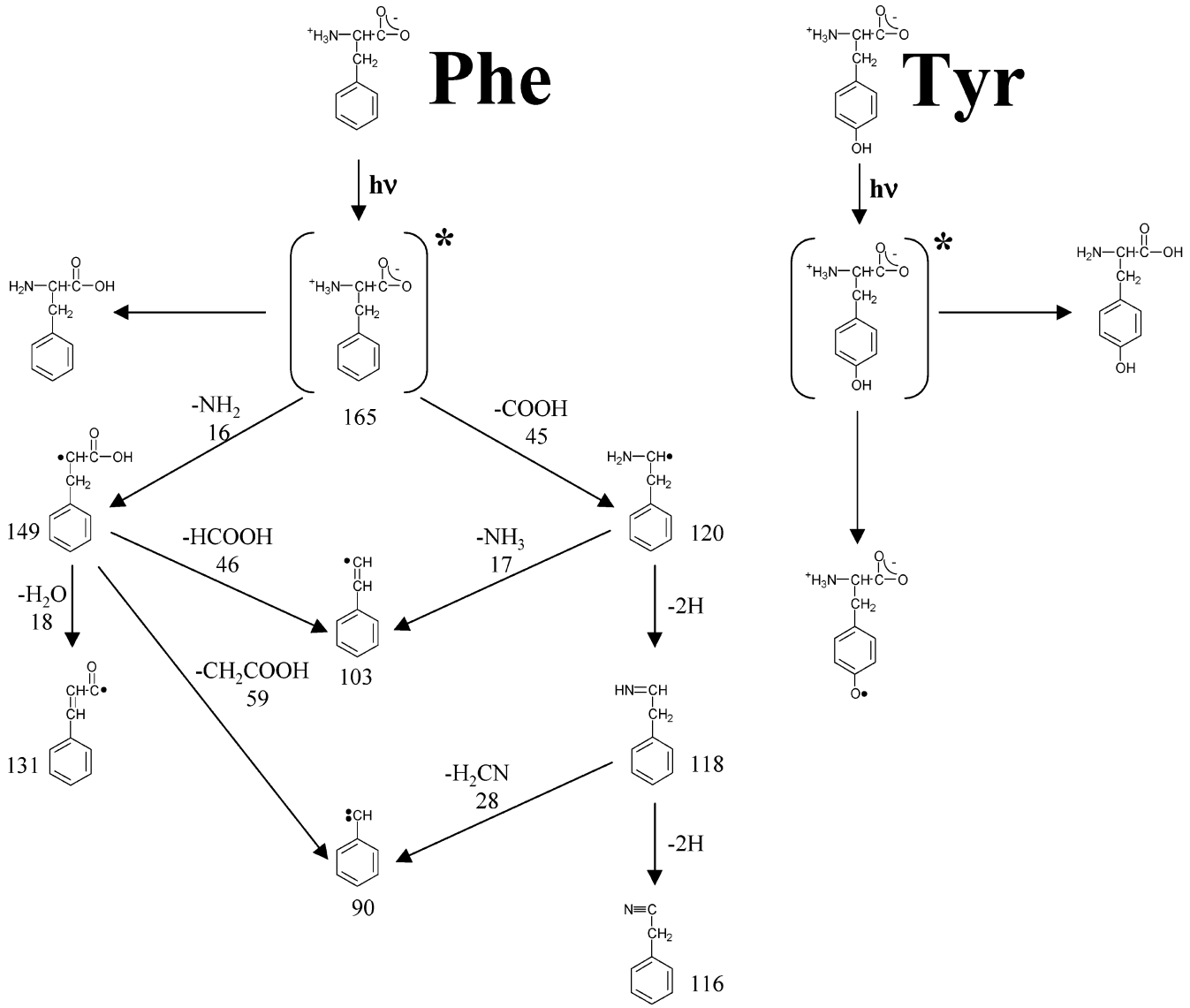

Figure 9. Qualitative scheme of the major processes initiated in phenylalanine (Phe) and tyrosine (Tyr) by soft X-ray irradiation. For phenylalanine, the molecular masses of the fragments are given.

Auger process leading to two valence holes within or near one atom) can result in a significant modification of the system, i.e., the breakage of a certain chemical bond. Note that this broken bond does not need to be located exactly at the point of the primary excitation. On the contrary, specific "weakest" bonds of the molecule are preferably affected, irrespective of the initial excitation point. Often, C−H, O−H, or N−H bonds represent these weakest bonds, and thus dehydrogenation occurs most readily. Radicals produced in this process, depending on their stability, either recombine with H atoms to restore parent molecules or decompose, triggering a chain of further radical reactions. A particular case of this dehydrogenation is the zwitterion → neutral molecule transition, which is associated with a proton transfer from initially protonated amino groups to carboxyl groups. This process takes place in both amino acids studied here (though it proceeds much faster for phenylalanine) and, in our context, is not classified as decomposition.

The experimental results presented above suggest that, in the case of an exposure of phenylalanine to soft X-rays, two major decomposition pathways are decarboxylation and deamination (i.e., scission of C−C and C−N bonds, leading to a release of gaseous carbon dioxide and ammonia, respectively). The radicals formed in these reactions may react further with neighboring molecules in a way similar to a radical polymerization. Alternatively, they can release low-molecular-weight fragments and thus transform into more stable species, such as benzyl or styryl radicals. Finally, since the decarboxylation and deamination products are substantially less polar and thus more volatile than the parent phenylalanine, they may be released to the gas phase.

The scheme in Figure 9 offers explanations for the origin of the major gaseous decomposition products of phenylalanine, as detected by mass spectrometry, and is consistent with the spectral changes observed in XPS and NEXAFS. The higher molecular mass peaks at $m/z = 90$, 103, 149, 131, and 116 amu observed in the mass spectra (see central panel of Figure 4) may be assigned to cations derived from toluene (benzyl radical), styrene (styryl radical), cinnamic acid, cinnamaldehyde, and phenylacetonitrile (see Figure 9). It is noted that we cannot conclude unambiguously where the respective cationic species are formed: in the solid state, at the solid/vacuum interface, in the gas phase, or in the ionizer of the mass spectrometer under electron impact. With a high level of confidence we assume that the initial steps (deamination and decarboxylation of phenylalanine) occur in the solid state as a result of the primary excitation and the ensuing relaxation processes. In contrast, a

fragmentation of the benzene ring, giving rise to mass spectral peaks at 48−52 amu (C_4H_x) and 60−65 amu (C_5H_x), hardly occurs under direct soft X-ray irradiation. Such peaks are characteristic fragments of aromatic molecules in electron impact mass spectra. Thus, along with phenyl radicals (73−78 amu), they are rather formed in the mass spectral ionizer by a fragmentation of species containing a benzene ring. On the other hand, we suggest that benzyl and styryl radicals, which are the most abundant higher molecular mass species in the residual gas, are also key intermediates in chemical transformations within the solid state. Note that, strictly speaking, the major MS peak at 90 amu is attributed to the benzylidene cation radical rather than to the much more stable benzyl cation, which should be observed at 91 amu. This may indicate that the registered benzylidene cations are formed in the MS ionizer from benzyl radicals, which actually desorb from the surface of the sample. As an overall effect of the irradiation, the solid phase of the phenylalanine sample is probably enriched with carbon-rich polymeric species composed of benzene rings fused to each other via $-CH_2-$ or $-CH{=}CH-$ bridges.

The behavior of tyrosine under irradiation is totally different as compared to that of phenylalanine. Its prominent stability against soft X-ray irradiation may be explained by a preferable formation of tyrosyl radicals as a stable intermediate (see Figure 9). Though some mass loss and modifications of functional groups occur in tyrosine upon prolonged irradiation, suggesting alternative decomposition pathways (such as dehydration of carboxyl groups), these alternative pathways are, to a great extent, suppressed.

5. Conclusions

Phenylalanine and tyrosine show drastically different behavior under exposure to soft X-ray radiation. Phenylalanine easily decomposes via several chemical pathways, among which deamination and decarboxylation are found to dominate. Benzyl and styryl radicals are key intermediates in the chain of decomposition reactions. In contrast, in the case of tyrosine, the formation of "molecular" tyrosyl radicals apparently suppresses alternative decomposition routes, thus providing a surprisingly high stability of the molecule against radiation.

Acknowledgment. We are grateful to the staff of BESSY and the ALS for technical support during the NEXAFS measurements. This work was supported by the German BMBF (Project Nos. 05 KS1VHA/3 and 05 KS1WW1/6) and the Fonds der Chemischen Industrie (M.G. and E.U.).

References and Notes

(1) *Desorption induced by electronic transitions, DIET-I*; Tolk, N. H., Traum, M. M., Tully, J. C., Madey, T. E., Eds.; Springer Series in Chemical Physics 24; Springer: Berlin, 1983.

(2) *DIET-II*; Brenig, W., Menzel, D., Eds.; Springer Series in Surface Science 4; Springer: Berlin, 1985.

(3) *DIET-III*; Stulen, R. H., Knotek, M. L., Eds.; Springer Series in Surface Science 13; Springer: Berlin, 1988.

(4) *DIET-IV*; Betz, G., Varga, P., Eds.; Springer Series in Surface Science 19; Springer: Berlin: 1990.

(5) *DIET-V*; Burns, A., Jennison, D., Stechel, E. B., Eds.; Springer Series in Surface Science 31; Springer: Berlin, 1993.

(6) Kempner, E. S. *J. Pharm. Sci.* **2001**, *90*, 1637.

(7) Crippa, P. R.; Tedeschi, R. A.; Vecli, A. *Int. J. Rad. Biol. Relat. Stud. Phys. Chem. Med.* **1974**, *25*, 497.

(8) Shields, H.; Gordy, W. *J. Phys. Chem.* **1958**, *62*, 789.

(9) Fasanella, E. L.; Gordy, W. *Proc. Natl. Acad. Sci. U.S.A.* **1969**, *62*, 299.

(10) McCormick, G.; Gordy, W. *J. Phys. Chem.* **1958**, *62*, 783.

(11) Fasanella, E. L.; Gordy, W. *Proc. Natl. Acad. Sci. U.S.A.* **1969**, *64*, 1.

(12) Box, H. C. *Annu. Rev. Nucl. Sci.* **1972**, *22*, 355.

(13) Box, H. C.; Budzinski, E. E.; Freund, H. G. *J. Chem. Phys.* **1974**, *61*, 2222.

(14) Box, H. C.; Freund, H. G. *Perspect. Cancer Res. Treat.* **1973**, 399.

(15) Box, H. C.; Budzinski, E. E. *J. Chem. Phys.* **1971**, *55*, 2446.

(16) Box, H. C. *Mult. Electron Reson. Spectrosc.* **1979**, 375.

(17) Benninghoven, A.; Lange, W.; Jirikowsky, M.; Holtkamp, D. *Surf. Sci.* **1982**, *123*, L721.

(18) Benninghoven, A.; Kempken, M.; Kluesener, P. *Surf. Sci.* **1988**, *206*, L927.

(19) Terhorst, M.; Kampwerth, G.; Niehuis, E.; Benninghoven, A. *J. Vac. Sci. Technol., A* **1992**, *10*, 3210.

(20) Abdoul-Carime, H.; Dugal, P. C.; Sanche, L. *Surf. Sci.* **2000**, *451*, 102.

(21) Herve du Penhoat, M.-A.; Huels, M. A.; Cloutier, P.; Jay-Gerin, J.-P.; Sanche, L. *J. Chem. Phys.* **2001**, *114*, 5755.

(22) Sanche, L. *J. Chim. Phys. Phys.-Chim. Biol.* **1997**, *94*, 216.

(23) Bozack, M. J.; Zhou, Y.; Worley, S. D. *J. Chem. Phys.* **1994**, *100*, 8392.

(24) Lin, S. D. *Radiat. Res.* **1974**, *59*, 521.

(25) Isaacson, M.; Johnson, D.; Crewe, A. V. *Radiat. Res.* **1973**, *55*, 205.

(26) Wade, R. H. *Ultramicroscopy* **1984**, *14*, 265.

(27) Burmeister, W. P. *Acta Crystallogr., Sect. D* **2000**, *56*, 328.

(28) Cheng, A.; Caffrey, M. *Biophys. J.* **1996**, *70*, 2212.

(29) Zubavichus, Y.; Fuchs, O.; Weinhardt, L.; Heske, C.; Umbach, E.; Denlinger, J. D.; Grunze, M. *Radiat. Res.* **2004**, *161*, 346.

(30) Coxon, P.; Krizek, J.; Humperson, M.; Wardell, I. R. M. *J. Electron Spectrosc. Relat. Phenom.* **1990**, *51*−*52*, 821.

(31) Powell, C. J. *Appl. Surf. Sci.* **1995**, *89*, 141.

(32) Clark, D. T.; Peeling, J.; Colling, L. *Biochim. Biophys. Acta* **1976**, *453*, 533.

(33) Zubavichus, Y.; Zharnikov, M.; Schaporenko, A.; Grunze, M. *J. Electron Spectrosc. Relat. Phenom.* **2004**, *134*, 25.

(34) Boese, J.; Osanna, A.; Jacobsen, C.; Kirz, J. *J. Electron Spectrosc. Relat. Phenom.* **1997**, *85*, 9.

(35) Kaznacheyev, K.; Osanna, A.; Jacobsen, C.; Plashkevych, O.; Vahtras, O.; Ågren, H.; Carravetta, V.; Hitchcock, A. P. *J. Phys. Chem. A* **2002**, *106*, 3153.

(36) Carravetta, V.; Plashkevych, O.; Ågren, H. *J. Chem. Phys.* **1998**, *109*, 1456.

(37) Francis, J. T.; Hitchcock, A. P. *J. Chem. Phys.* **1992**, *96*, 6598.

(38) Urquhart, S. G.; Ade, H. *J. Phys. Chem. B* **2002**, *106*, 8531.

(39) Gordon, M. L.; Cooper, G.; Morin, C.; Araki, T.; Turci, C.; Kaznacheyev, K.; Hitchcock, A. P. *J. Phys. Chem. A* **2003**, *107*, 6144.

(40) Sodhi, R. N. S.; Brion, C. E. *J. Electron Spectrosc. Relat. Phenom.* **1985**, *36*, 187.

(41) Turci, C. C.; Urquhart, S. G.; Hitchcock, A. P. *Can J. Chem.* **1996**, *74*, 851.

(42) Weissbuch, I.; Frolow, F.; Addadi, L.; Lahav, M.; Leiserowitz, L. *J. Am. Chem. Soc.* **1990**, *112*, 7718.

(43) Frey, M. N.; Koetzle, T. F.; Lehmann, M. S.; Hamilton, W. C. *J. Chem. Phys.* **1973**, *58*, 2547.

(44) Myneni, S.; Luo, Y.; Näslund, L. Å.; Cavalleri, M.; Ojamäe, L.; Ogasawara, H.; Pelmenschikov, A.; Wernet, Ph.; Väterlein, P.; Heske, C.; Hussain, Z.; Pettersson, L. G. M.; Nilsson, A. *J. Phys.: Condens. Matter* **2002**, *14*, L213.

(45) Biemann, K.; Seibl, J.; Gapp, F. *J. Am. Chem. Soc.* **1961**, *83*, 3795.

(46) Hulsebosch, R. J.; van den Brink, J. S.; Nieuwenhuis, S. A. M.; Gast, P.; Raap, J.; Lugtenburg, J.; Hoff, A. J. *J. Am. Chem. Soc.* **1997**, *119*, 8685.

(47) Magnuson, A.; Berglund, H.; Korall, P.; Hammarström, L.; Åkermark, B.; Styring, S.; Sun, L. *J. Am. Chem. Soc.* **1997**, *119*, 10720.

(48) Himo, F.; Siegbahn, P. E. M. *Chem. Rev.* **2003**, *103*, 2421.

(49) Sealy, R. C.; Harman, L.; West, P. R.; Masont, R. P. *J. Am. Chem. Soc.* **1985**, *107*, 3401.

(50) Butler, J.; Land, E. J.; Pruetz, W. A.; Swallow, A. J. *Biochim. Biophys. Acta* **1982**, *705*, 150.